Clinical and Radiological Characteristics of Intracranial Artery Dissection Using Recently Proposed Diagnostic Criteria

Yuki Nakamura, MD,*,† Yoshitaka Yamaguchi, MD, PhD,* Naoki Makita, MD,*,‡ Yoshiaki Morita, MD, PhD,§ Toshihiro Ide, MD,* Shinichi Wada, MD,* Tadataka Mizoguchi, MD,* Hajime Ikenouchi, MD,* Kaori Miwa, MD, PhD,* Kenichiro Yi, MD,* Kenichi Irie, MD,* Shun Shimohama, MD, PhD,† Masafumi Ihara, MD, PhD,¶ Kazunori Toyoda, MD, PhD,* and Masatoshi Koga, MD, PhD*

Background: Data on the clinical and radiological characteristics of intracranial artery dissection (IAD) have remained limited. Our purpose was to reveal the clinical and radiological characteristics of IAD according to diagnostic criteria for IAD as recently reported by a group of international experts. *Methods:* Patients were retrospectively enrolled using a prospective single-center stroke registry between 2011 and 2016. Baseline characteristics and radiological findings including conventional magnetic resonance imaging (MRI) sequences, magnetic resonance angiography (MRA), high-resolution 3-dimensional T1-weighted imaging (HR-3D-T1WI), and digital subtraction angiography were reviewed. We performed statistical comparisons to determine which findings from which modalities are useful. *Results:* We identified 118 patients with suspected artery dissection, with 64 patients (median age, 51 [interquartile range, 45-56) years; 16 women) finally meeting the criteria for definite (n = 47), probable (n = 15), or possible (n = 2) idiopathic IAD. Ischemic stroke alone was found in 31 patients (48%) on admission. There were 36 patients (56%) suffering from hypertension and 39 (61%) with smoking history. The vertebral artery alone was the most affected in 42 patients (66%). Intramural hematoma (IMH) was more frequently detected on HR-3D-T1WI than on conventional MRI/MRA (odds ratio, 4.72; 95% confidence interval, 1.71-13.00). In 54 patients (84%), the modified Rankin Scale score after 3 months was 0-1. *Conclusions:* Male dominance and age at IAD onset were similar to previous studies, and more than half had hypertension and smoking history. We confirmed that HR-3D-T1WI is useful for detecting IMH in the diagnostic criteria.

Key Words: Criteria—high-resolution magnetic resonance imaging—intracranial artery dissection—intramural hematoma—stroke

From the *Department of Cerebrovascular Medicine, National Cerebral and Cardiovascular Center, Suita, Japan; †Department of Neurology, Sapporo Medical University School of Medicine, Sapporo, Japan; ‡Department of Neurology, Kyoto Prefectural University of Medicine, Kyoto, Japan; §Department of Radiology, National Cerebral and Cardiovascular Center, Suita, Japan; and ¶Department of Neurology, National Cerebral and Cardiovascular Center, Suita, Japan.

Received September 25, 2018; revision received December 28, 2018; accepted February 16, 2019.

Financial Disclosure: This study was funded by Grant-in-Aid for Scientific Research (C), JSPS KAKENHI Grant Number 16K09485. Funders played no role in the study design, collection, analysis or interpretation of data, or writing of this manuscript.

Address correspondence to Yoshitaka Yamaguchi, MD, PhD, Department of Cerebrovascular Medicine, National Cerebral and Cardiovascular Center, 5-7-1 Fujishiro-dai, Suita, Osaka 565-8565, Japan. E-mail: y.yamaguchi830@gmail.com.

1052-3057/$ - see front matter

https://doi.org/10.1016/j.jstrokecerebrovasdis.2019.02.019

Introduction

Intracranial artery dissection (IAD) is increasingly recognized as an important cause of stroke in young and middle-aged adults.[1-3] Diagnosis of IAD is difficult, as widely recognized, standard radiological criteria remain lacking.[4] Details of inclusion and exclusion criteria for IAD have differed between studies.[5-8]

Many researchers have tried to report the radiological characteristics of patients with IAD.[9,10] Because high-resolution magnetic resonance imaging (HR-MRI) has improved wall visualization compared with conventional MRI[11] and allows identification of intramural hematoma (IMH),[12] this modality appears important for evaluating dissection of the arterial wall. However, no consensus has been reached regarding diagnostic criteria and imaging. This problem has made multicenter, prospective, and randomized trials for patients with IAD difficult to conduct.

A group of international experts on IAD recently provided a consensus statement and criteria for the diagnosis of IAD (Table 1).[13] These criteria included image diagnostic criteria based not only on the results of vessel wall imaging from one-off examinations, but also on changes in imaging results between baseline and follow-up.

These new criteria appear to resolve the problem of diagnosing IAD. However, little data have been reported showing the features of IAD based on these new criteria. The present study aimed to clarify the clinical and radiological characteristics of IAD based on the criteria.

Table 1. *Grading of imaging diagnostic criteria for evidence of intracranial artery dissection*

Definite IAD
Stenosis or occlusion of an intracranial artery secondarily developing towards fusiform or irregular aneurysmal dilation at a non-branching site
Intramural hematoma, intimal flap, or double lumen
Pathological confirmation of intracranial artery dissection
Probable IAD
Fusiform or irregular aneurysmal dilation and focal, long filiform, or irregular stenosis (so-called pearl-and-string sign) without subarachnoid hemorrhage, or still present > 1 month after subarachnoid hemorrhage
Fusiform or irregular aneurysmal dilation at non-branching site with rapid change in morphology (increase or reduction in size, or subsequent appearance of stenosis)
Possible IAD
Fusiform or irregular aneurysmal dilation at non−branching site without change in morphology on repeated imaging within 6-12 months after first imaging
Long filiform or irregular stenosis of an intracranial artery, with reduction in size or disappearance over time

Abbreviation: IAD, intracranial artery dissection.

Materials and methods

Subjects

This retrospective study was performed using the prospective National Cerebral and Cardiovascular Center stroke registry (Clinical Trial.gov: NCT02251665). This registry included around 10,000 patients admitted to our department between March 2011 and November 2016. This registry did not contain patients with IAD admitted to the Department of Neurosurgery for the purpose of surgical procedures, including endovascular therapy. We extracted patients with suspected artery dissection in this registry. The registered diagnosis in each case was made mainly by the team of doctors in charge, and also by the consensus decision of our department. We excluded patients who showed extracranial artery dissection or had pre-existing diagnoses of arteritis/vasculitis/arteriosclerosis disease or traumatic, iatrogenic, or chronic (>1 month since onset) IAD. For the remaining patients, radiological findings were reviewed. Only those patients who met the new criteria for IAD were finally included in our study population. Baseline patient characteristics including age, sex, comorbid conditions (hypertension, dyslipidemia, and diabetes mellitus), smoking history, prior medication, affected arteries, stroke subtype, clinical presentation on admission, date of onset, and modified Rankin Scale score at 3 months after onset were collected from our database. Hypertension, dyslipidemia, and diabetes mellitus were defined according to medical records.[8] Brainstem compressive symptoms were defined when dissecting aneurysmal dilation or basilar artery dissections compressed the brainstem and showed mass effects causing brainstem dysfunction. If a patient showed more than one dissection, only the artery considered to have contributed most to patient symptoms was used to classify the diagnostic grade.

Institutional Ethics Approval

According to the standard ethical guidelines for retrospective clinical research in Japan, the requirement for informed consent was waived. Ethics approval was obtained from the local ethics committee at our center (approval number, M28-054-3).

MRI

All patients underwent conventional MRI performed using a 1.5-T MRI scanner (MAGNETOM Sonata; Siemens Healthcare, Erlangen, Germany) or 3.0-T MRI scanner (MAGNETOM Verio 3T or MAGNETOM Spectra 3T; Siemens Healthcare). In addition, we adapted the high-resolution 3-dimensional T1-weighted imaging (HR-3D-T1WI) as HR-MRI using a 3.0-T MRI scanner. HR-3D-T1WI is one of the efficient 3-dimensional-turbo spin echo (3D-TSE) techniques that were originally applied for whole-brain imaging.[14] The 3D-TSE sequence adapts

variable refocusing flip angle and nonselective radiofrequency pulses.[15] Moreover, HR-3D-T1WI has proven useful thanks to the excellent arterial wall imaging achieved using the black blood technique[16] and good correlation with contrast-enhanced MR angiography (MRA) methods.[17] HD-3D-T1WI generally uses fat-suppression technology. The team of doctors in charge judged the indications for HR-3D-T1WI evaluations.

The conventional MRI protocol included diffusion-weighted imaging, fluid-attenuated inversion recovery, T2*-weighted imaging, and 3-dimensional time-of-flight MRA. Generally, HR-MRI studies were performed without a definite diagnosis based only on conventional MRI (C-MRI)/MRA. The protocol parameters for C-MRI/MRA and HR-3D-T1WI are shown in Table 2.

We defined IMH as eccentric-bright MRA (axial source images) or HR-3D-T1WI elements showing >200% of the signal intensity of sternocleidomastoid muscle[18-20] in the arterial wall, often appearing as crescent-shaped thickening. The lipid core, an important component of atheromatous plaque, can be distinguished from IMH because it appears as hypointensity on fat-suppressed T1WI.[21] An intimal flap was defined as an arterial vessel layer crossing the lumen.[22] A double lumen was defined when vascular flow was seen in both true and false arterial lumina.[23] Aneurysmal dilatation was defined when the arterial vessel diameter was 1.5 times the width of the normal-appearing artery.[24] Examples are shown in Figure 1A-H.

Digital Subtraction Angiography (DSA)

Indications for DSA in each patient were determined by the team of attending physicians. We evaluated representative DSA findings considered to indicate arterial dissection, as follows. We categorized fusiform or irregular aneurysmal dilation if the ratio between the diameter of

Table 2. *Acquisition parameters for C-MRI/MRA, and HR-3D-T1WI*

a. MAGNETOM Spectra 3T (Siemens Healthcare)

	DWI	FLAIR	T2*	MRA	HR-3D-T1WI
TR/TE (ms)	5000/82	12000/114	550/12	25/3.69	550/22
Matrix	128 × 104	320 × 189	320 × 182	384 × 261	320 × 320
FOV (mm)	230	230	230	200	200
Section thickness (mm)	5	5	4	0.6	0.6
Intersection gap (mm)	1	1	2	N/A	N/A
Other parameters: DWI (b-values, 0 s/mm^2 and 1000 s/mm^2), FLAIR (TI, 2800 ms), MRA (FA = 18°, acquisition time = 6 min 15 s), HR-3D-T1WI (FA variable; slices = 52, acquisition time = 6 min 27 s)					

b. MAGNETOM Verio 3T (Siemens Healthcare)

	DWI	FLAIR	T2*	MRA	HR-3D-T1WI
TR/TE (ms)	6300/80	12000/94	550/12	25/3.69	450/27
Matrix	128 × 115	320 × 182	320 × 260	384 × 261	384 × 261
FOV (mm)	230	230	230	200	200
Section thickness (mm)	5	5	4	0.6	0.6
Intersection gap (mm)	1	1	2	N/A	N/A
Other parameters: DWI (b-values, 0 s/mm2 and 1000 s/mm2), FLAIR (TI, 2700 ms), MRA (FA = 18°, acquisition time = 6 min 15 s), HR-3D-T1WI (FA variable; 51 slices; acquisition time, 6 min 45 s)					

c. MAGNETOM Sonata 1.5T (Siemens Healthcare)

	DWI	FLAIR	T2*	MRA
TR/TE (ms)	3000/72	9000/119	700/20	37/7.15
Matrix	128 × 128	256 × 224	256 × 224	514 × 224
FOV (mm)	230	230	230	200
Section thickness (mm)	4	5	5	0.6
Intersection gap (mm)	2	1	1	N/A
Other parameters: DWI (b-values, 0 s/mm^2 and 1000 s/mm^2), FLAIR (TI 2500 ms), MRA (FA = 25°, acquisition time = 6 min 33 s)				

Abbreviations: C-MRI/MRA, conventional magnetic resonance imaging and magnetic resonance angiography; DSA, digital subtraction angiography; DWI, diffusion-weighted imaging; FA, flip angle; FLAIR, fluid-attenuated inversion recovery; FOV, field of view; HR-3D-T1WI, high-resolution 3-dimensional T1-weighted imaging; MRA, 3-dimensional time-of-flight magnetic resonance angiography; N/A, not available; T2*, T2*-weighted imaging; TE, echo time; TR, repetition time.

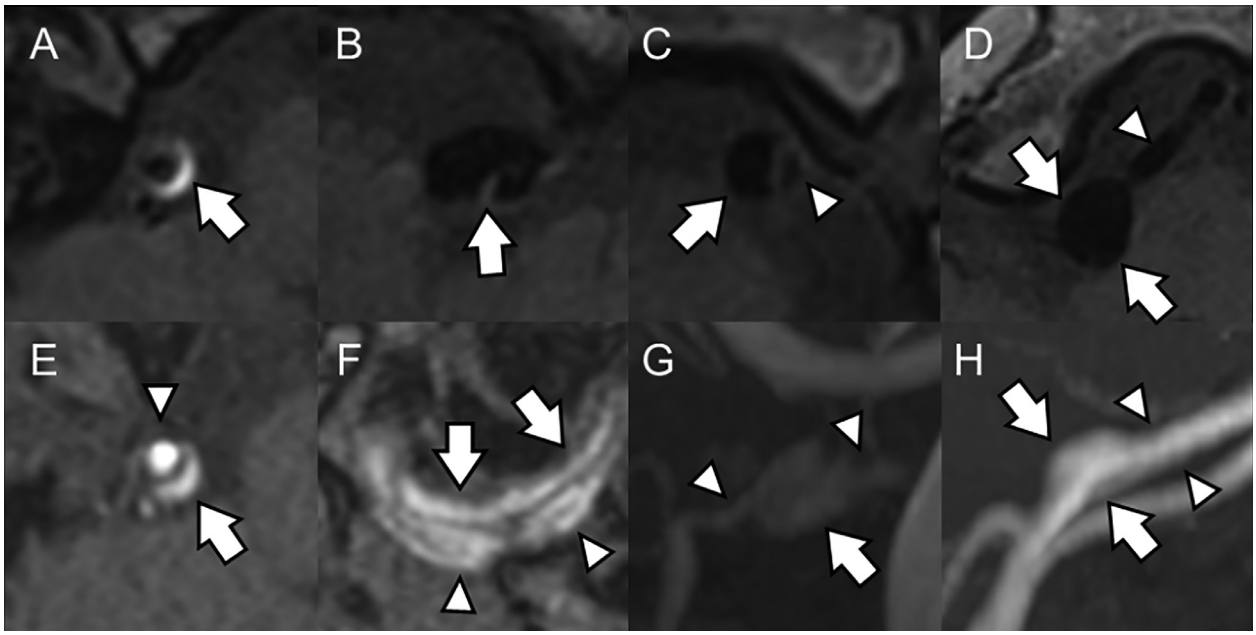

Figure 1. *Vessel images suggesting intracranial artery dissection. High-resolution 3-dimensional T1-weighted imaging shows: (A) intramural hematoma of the right vertebral artery (arrow indicates eccentric bright elements >200% of signal intensity of the sternocleidomastoid muscle); (B) intimal flap of the left vertebral artery (arrow indicates arterial vessel layer crossing the lumen); (C) double lumen of the left vertebral artery (arrow and arrowhead); and (D) aneurysmal dilatation of the right vertebral artery (arrow indicates arterial vessel dilatation, representing a diameter 1.5 times the width of the normal-appearing artery [arrowheads]). Magnetic resonance angiography imaging shows: (E) intramural hematoma (arrow) and lumen (arrowhead) of the right vertebral artery; (F) double lumen of the right vertebral artery (arrows indicate true lumen and arrowheads indicate false lumen); (G) pearl-and-string sign of the right vertebral artery (arrow indicates "pearl" part, arrowheads indicate "string" part); and (H) aneurysmal dilatation of the right vertebral artery (arrow indicates aneurysmal dilatation, arrowheads indicate normal-appearing artery).*

the aneurysm and that of the normal-looking artery was >1.5.[24] The string sign included luminal narrowing >30%.[24] If the lumen gradually tapered and ended in total occlusion, we included tapered occlusion.[5,24,25] The combined pattern was categorized as pearl-and-string sign when aneurysmal dilation was seen with stenosis on both sides. Pearl sign included dilation without stenosis, not including aneurysm.[5,25] If the pearl-and-string sign accompanied tapered occlusion, we considered this as total occlusion with proximal distension. When intraaneurysmal contrast retention was seen even in the late or venous phase of angiography, we included retention of contrast.[26] We also defined an intimal flap and a double lumen in the same manner as for C-MRI/MRA.[22,23] Examples are shown in Figure 2A-G.

Imaging Analysis

Three vascular neurologists (YN, NM, and YY) checked all images to identify specific radiological findings of IAD according to the criteria.[13] We classified radiological findings for each patient as definite, probable, possible dissection, or undiagnosed IAD. The neurologists were blinded to patient characteristics. In cases of disagreement regarding the diagnosis of IAD or radiological findings, the neurologists re-evaluated the radiological findings together and reached a final consensus decision. After this evaluation, three other vascular neurologists (TM, HI, and KM) performed a re-evaluation (definite, probable, possible dissection, or undiagnosed IAD) in a random sample of 20% and inter-rater reliability was calculated. When patients underwent each imaging modality for the first time after admission, we defined this as the initial imaging in each radiological modality. The timing of follow-up imaging depended on the decisions of each physician. We compared radiological findings between initial and follow-up imaging in the same modality according to the proposed grading of imaging criteria.[13] We defined rapid changes in morphology[13] as either (1) fusiform or irregular aneurysmal dilation at a non−branching site with increased or reduced size, or subsequent appearance of stenosis, or (2) long filiform or irregular stenosis with increased or reduced size, or subsequent appearance of aneurysmal dilation, confirmed on both initial imaging and follow-up imaging in the same modality (C-MRI/MRA or DSA). We did not evaluate rapid change in morphology using HR-3D-T1WI, because HR-3D-T1WI could not be extracted as a 3-dimensional image and evaluation of stereoscopic changes was predicted to often be difficult.

Statistical Analysis

We performed multivariable logistic regression analysis to clarify which modalities (C-MRI/MRA, HR-3D-T1WI, and DSA) were useful for detecting each radiological

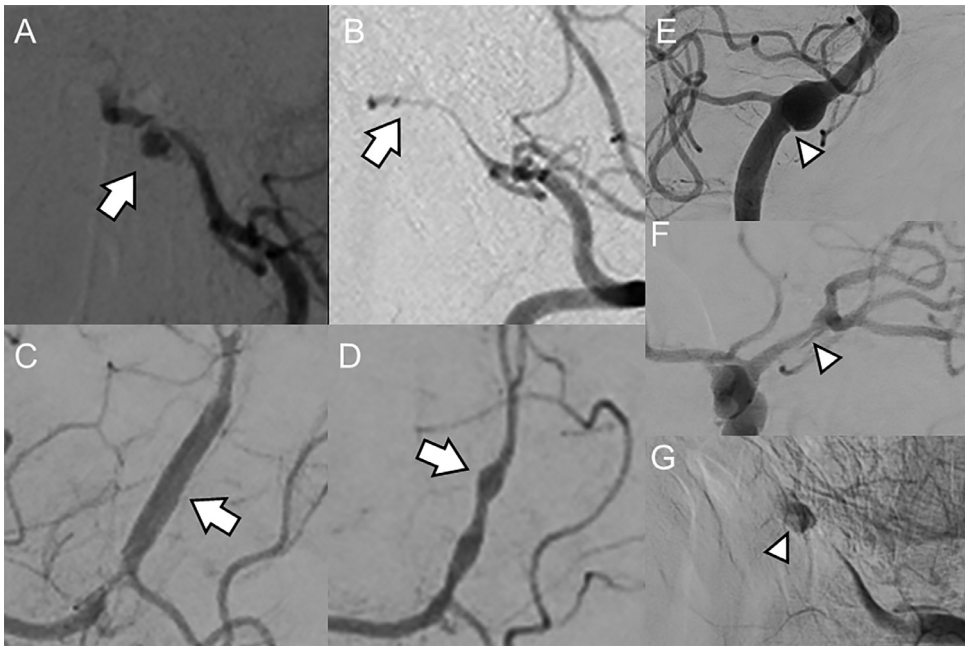

Figure 2. *Representative digital subtraction angiography findings of intracranial artery dissection. (A) Irregular aneurysmal dilation at a non-branching site of the right vertebral artery. (B) Arrow points to secondarily developed stenosis (occlusion) at a non−branching site of the right vertebral artery. (C) Fusiform aneurysmal dilation at a non-branching site of the right anterior cerebral artery. (D) Arrow points to subsequent appearance of stenosis (pearl-and-string sign) of the right anterior cerebral artery. (E) Intimal flap of the left vertebral artery (arrowhead). (F) Double lumen of the left middle cerebral artery (arrowhead). G) Retention of contrast in the left vertebral artery (arrowhead). A and B are from the same patient, at an interval of 1 week. C and D are from the same patient, at an interval of 2 weeks.*

finding. When we evaluated a radiological finding using 2 modalities, we processed paired comparisons. When we evaluated radiological findings using 3 modalities to compare the diagnostic contributions of each finding in the 3 modalities, we used dummy variable and processed-paired comparisons[27] (C-MRI/MRA versus HR-3D-T1WI, C-MRI/MRA versus DSA, HR-3D-T1WI versus DSA). We adopted multiple evaluations in different radiological modalities as explanatory variables for all multivariable logistic regression analyses, because the combination of imaging modalities used influences the findings obtained.[28] Our study also needed to determine whether evaluation in multiple radiological modalities for 1 patient influenced the proportion of the presence of each radiological characteristic. When we performed multivariable logistic regression analysis at initial imaging, we adopted the interval from symptom onset to initial imaging as an explanatory variable. When we performed multivariable logistic regression analysis for comparisons between initial and follow-up imaging, we adopted the interval from initial to follow-up imaging as an explanatory variable. We selected this time period as an explanatory variable because radiological findings suggesting IAD varied depending on the timing of symptom onset.[5,10] None of the data on the intervals from onset to performance of each imaging modality were missing. As increasing other explanatory variables carries a risk of making the statistical model unstable and factors suggested as relevant from past reports have not yet become well known, we finally selected these 2 explanatory variables. All reported probability values were 2-sided, and values of $P < .05$ were considered statistically significant. To reduce the risk of type I errors, the Bonferroni correction was used to adjust P values when we performed multiple statistical tests between the 3 groups ($P < .016$). The weighted kappa was used to evaluate the inter-rater reliability of the diagnosis of IAD.

All statistical analyses were performed using R for Windows version 3.2.2 software (www.r-project.org).

Results

A retrospective review of patients with suspected artery dissection identified 118 patients in this registry. Finally, 64 patients met the new criteria for IAD and were included in the study population. Inter-rater reliability of diagnosis of IAD was excellent (weighted kappa = 0.95). Baseline characteristics of the 64 patients are shown in Table 3. Median age at occurrence was 51 years, and a male preponderance (48 patients, 75%) was seen, with more than half of the patients having histories of both hypertension (56%) and smoking (61%). Four patients (6%) were using antithrombotic drugs on admission. Ischemic stroke was the most common subtype (48%), followed by patients with nonstroke onset (41%). All nonstroke onset patients except one reported head or neck pain. Forty-eight patients (75%) had headache or neck pain on admission. No patient had compressive symptoms related to mass effects such as progressive brainstem

Table 3. *Demographic characteristics of patients with intracranial artery dissection*

	Patients diagnosed with IAD (n = 64)
Age (years), median (IQR)	51 (45-56)
Woman, n (%)	16 (25)
Antithrombotic use on admission, n (%)	4 (6)
Vascular risk factors, n (%)	
Hypertension	36 (56)
Dyslipidemia	22 (34)
Diabetes	2 (3)
Past/current smoking history	39 (61)
Current smoker	21 (33)
Past smoker	18 (28)
Systolic BP (mmHg), mean ± SD	156 ± 24
Diastolic BP (mmHg), median (IQR)	95 (82-102)
Clinical presentation on admission, n (%)	
Head or neck pain	48 (75)
Compressive symptoms	0 (0)
NIHSS on admission of stroke patients, median (IQR)	2 (1-4.5)
Initial stroke subtype, n (%)	
Stroke onset	38 (59)
Ischemic stroke alone	31 (48)
Non-stroke onset	26 (41)
Affected (dissected) artery, n (%)	
Posterior circulation	49 (77)
Vertebral artery	42 (66)
Anterior circulation	15 (23)

Abbreviations: BP, blood pressure; IAD, intracranial artery dissection; IQR, interquartile range; NIHSS, National Institutes of Health stroke scale; SD, standard deviation.

Total number of stroke patients was 38.

Continuous variables are presented as mean ± standard deviation, median (interquartile range: 25th-75th percentile), absolute frequency or percentage (%), as appropriate.

ischemia or cranial nerve deficits. Median National Institutes of Health Stroke Scale score in stroke patients was 2 (interquartile range [IQR], 1-4.5). Dissection was more common in the posterior circulation than in the anterior circulation (77% versus 23%), and the vertebral artery was most affected.

Initial grading of imaging diagnostic criteria is shown in Table 4. We evaluated 64 patients by C-MRI/MRA, 50 by HR-3D-T1WI, and 51 by DSA at the initial imaging. Using the same modality, we were able to follow-up all 64 patients who initially underwent C-MRI/MRA, all 34 patients who initially underwent HR-3D-T1WI, and all 20 patients who initially underwent DSA at the subacute stage. The timings of acquisition for each imaging modality from symptom onset are shown in Table 5. IAD was definite in 47 cases, probable in 15 cases, and possible in 2 cases (Table 6). Thirteen patients (20%) were not diagnosed as having IAD from the first imaging. However, follow-up imaging contributed to the diagnosis of IAD in all patients.

Radiological findings with each modality are shown in Table 7. When we focused on HR-3D-T1WI, IMH was identified in 26 patients (52%) from the initial image and in 20 patients (59%) from follow-up images. Four patients showed the presence of IMH only on repeated HR-3D-T1WI studies.

We compared initial and follow-up imaging with the same modality. IMH was found with at least one modality in 29 patients on the initial image and in 24 patients on follow-up imaging. Compared with imaging modalities, IMH was more frequently observed on HR-3D-T1WI than on C-MRI/MRA (initial image: odds ratio, 4.72; 95% confidence interval, 1.71-13.00; Table 8). Three patients were diagnosed with IAD only when detecting IMH on follow-up imaging (Table 6). No other significant differences were observed in rate of double lumen/intimal flap, fusiform or irregular aneurysmal dilation, pearl-and-string sign, or string sign.

When we compared differences between primary and subsequent shape of the dissected artery, rapid change in morphology was confirmed in 46 patients (72%) on C-MRI/MRA and in 13 patients (65%) on DSA (Table 7). Forty-seven patients showed rapid changes in morphology on either C-MRI/MRA or DSA. No significant difference was observed between C-MRI/MRA and DSA (Table 8). Four patients were diagnosed with IAD based solely on a finding of a rapid change in morphology (Table 6).

Regarding the clinical outcome, median modified Rankin Scale at 3 months after onset was 0 (IQR, 0-1) for 64 IAD patients and 1 (IQR, 0-1.75) for stroke patients

Table 4. *Initial grading under different imaging diagnostic criteria*

Grading	C-MRI/MRA (n = 64)	HR-3D-T1WI (n = 50)	DSA (n = 51)	All modalities combined (n = 64)
Definite, n (%)	12 (19)	33 (66)	6 (12)	36 (61)
Probable, n (%)	10 (15)	0 (0)	16 (31)	12 (19)
Possible, n (%)	0 (0)	0 (0)	0 (0)	0 (0)
Undiagnosed, n (%)	42 (66)	17 (34)	29 (57)	13 (20)

Abbreviations: C-MRI/MRA, conventional magnetic resonance imaging and magnetic resonance angiography; DSA, digital subtraction angiography; HR-3D-T1WI, high-resolution 3-dimensional T1-weighted imaging.

Table 5. *Intervals from symptom onset to performance of each imaging modality*

	Onset to initial imaging (days)	Onset to follow-up imaging (days)	Interval between initial and follow-up (days)
C-MRI/MRA	4.0 (1.0-9.0)	17.5 (12.0-35.0)	13.0 (7.0-27.3)
HD-3D-T1WI	10.0 (7.5-13.5)	24.5 (16.0-39.8)	8.0 (6.0-26.5)
DSA	8.0 (3.0-12.0)	24.0 (17.8-59.8)	17.5 (14.0-48.8)

Abbreviations: C-MRI/MRA, conventional magnetic resonance imaging and magnetic resonance angiography; DSA, digital subtraction angiography; HR-3D-T1WI, high-resolution 3-dimensional T1-weighted imaging.
Descriptive statistics are presented as median value (25th-75th percentile).

(Table 9). A modified Rankin Scale score ≤1 at 3 months was observed in 54 of 64 IAD patients (84%).

Discussion

This retrospective study investigated clinical characteristics and radiological features of patients with IAD using the recently proposed diagnostic criteria. Our results showed a male predominance and middle-aged onset, supporting previous reports.[5,29] More than half of the IAD cases showed a medical history of hypertension or smoking. The rate of observed IMH was significantly higher on HR-3D-T1WI than on C-MRI/MRA.

Relatively little data have been accumulated in relation to IAD compared with cervical artery dissection, and incidences of IAD might differ between Asian and Western countries.[13] Non−high-resolution vascular imaging might have been one important reason for not detecting specific findings of IAD, such as IMH, intimal flap, and double lumen. For example, probably due to the quality of vascular imaging, the prevalence of anterior cerebral artery dissection varied markedly between studies,[8,30,31] before the recently proposed diagnostic criteria were published.

In our study, more than half of the IAD patients had hypertension or smoking history, suggesting these as potential risk factors for IAD. Hypertension may increase the risk of IAD compared with extracranial artery dissection.[32] A recent meta-analysis of studies into anterior cerebral artery dissection reported hypertension in 60% of cases and diabetes mellitus in 2%.[33] However, part of the risk factor data was missing. Experimental studies have shown that hypertension damages the normal endothelium and causes endothelial dysfunction. Recent studies have also identified new evidence of endothelial dysfunction in human hypertension.[34] Smoking has a pathologic effect on the arterial wall.[35] A subanalysis of the largest case series of cervical artery dissection suggested an association between current smoking and cervical artery

Table 6. *Grading of imaging diagnostic criteria and grading change at follow-up imaging in 64 patients with intracranial artery dissection*

a. Grading change at follow-up imaging (n = 64)

Grading	Initial imaging only, n (%)	Initial and follow-up imaging, n (%)
Definite	36 (61)	47 (73)
Probable	12 (19)	15 (23)
Possible	0 (0)	2 (4)
Undiagnosed	13 (20)	Not applicable

b. Grading change of imaging diagnostic criteria and radiological findings in 13 initially undiagnosed intracranial artery dissection patients

Radiological findings with grade changed at follow-up imaging	n	Grading change of imaging diagnostic criteria
Fusiform or irregular aneurysmal dilation at a non−branching site with rapid change in morphology	4	Undiagnosed → Probable
Intramural hematoma	3	Undiagnosed → Definite
Double lumen or intimal flap	2	Undiagnosed → Definite
Pearl-and-string sign	2	Undiagnosed → Probable
Fusiform or irregular aneurysmal dilation at non−branching sites without changes in morphology on repeated imaging	2	Undiagnosed → Possible

Table 7. *Representative radiological findings and imaging modalities*

a. C-MRI/MRA (Initial imaging, n = 64, follow-up imaging, n = 64)

	Initial	Follow-up
Intramural hematoma, n (%)	9 (14)	14 (22)
Double lumen or intimal flap, n (%)	6 (9)	5 (8)
Fusiform or irregular aneurysmal dilation, n (%)	24 (38)	21 (33)
Pearl-and-string sign, n (%)	12 (19)	10 (16)
Comparison between initial and follow-up imaging (n = 64)		
Rapid change in morphology, n (%)		46 (72)
Fusiform or irregular aneurysmal dilation at a non−branching site (increased or reduced size, or subsequent appearance of stenosis), n (%)		18 (28)
Long fusiform or irregular stenosis (increased or reduced size, or subsequent appearance of aneurysmal dilation), n (%)		28 (44)

b. HR-3D-T1WI (initial imaging, n = 50, follow-up imaging, n = 34)

	Initial	Follow-up
Intramural hematoma, n (%)	26 (52)	20 (59)
Double lumen or intimal flap, n (%)	9 (18)	6 (18)
Fusiform or irregular aneurysmal dilation, n (%)	18 (36)	16 (47)

c. DSA (Initial imaging, n = 51, follow-up imaging, n = 20)

	Initial	Follow-up
Double lumen or intimal flap, n (%)	6 (12)	3 (15)
Fusiform or irregular aneurysmal dilation, n (%)	19 (37)	3 (15)
Pearl-and-string sign, n (%)	18 (35)	6 (30)
Comparison between initial and follow-up imaging (n = 20)		
Rapid change in morphology, n (%)		13 (65)
Fusiform or irregular aneurysmal dilation at a non−branching site (increased or reduced size, or subsequent appearance of stenosis), n (%)		5 (25)
Long fusiform or irregular stenosis (increased or reduced size, or subsequent appearance of aneurysmal dilation), n (%)		8 (40)

Abbreviations: C-MRI/MRA, conventional magnetic resonance imaging and magnetic resonance angiography; DSA, digital subtraction angiography; HR-3D-T1WI, high-resolution 3-dimensional T1-weighted imaging.

We omitted the data of string sign in C-MRI/MRA.

We omitted the data of string sign, pearl sign, retention of contrast, tapered occlusion, and total occlusion with proximal distension in DSA.

dissection with cerebral ischemia in referents extracted from population-based surveys.[36] From these points of view, hypertension and smoking may increase the risk of IAD. Nevertheless, no reports have confirmed smoking as a risk factor for the onset of IAD. True putative-risk factors for IAD are not well known.[13] However, although detailed mechanisms have been unclear, both hypertension and smoking may damage the vascular endothelium, resulting in a dissection-prone situation.

In this study, 13 patients (20%) could not be diagnosed with IAD from the initial imaging among those patients. Scant data are available regarding the importance of follow-up imaging for diagnosing IAD.[5,10] Follow-up imaging was performed to observe dissecting aneurysm or changes in primary-vessel shape after diagnosing IAD.[5,37] Intracranial arteries show small diameter and winding, which increases the difficulty of distinguishing between IAD and other diseases such as arteriosclerotic change on first imaging. Some studies have reported that segmental stenosis, occlusion, and aneurysmal dilatation are often seen in IAD,[5,7,25] but these findings are not specific to IAD. Because morphological changes are important features for IAD, and additional radiological information is required to ensure the diagnosis of IAD, the new criteria[13] emphasize repeated imaging.

On follow-up, rapid changes in morphology and presence of IMH contributed to diagnosis of IAD, and re-examination including these 2 findings was important for diagnosing IAD in more than one-fifth of IAD patients in this study. A total of 47 cases showed a rapid change in morphology and 24 cases had IMH in the follow-up study. Meanwhile, one of the studies using HR-MRI

Table 8. *Multivariable logistic regression analysis for associations between each imaging modality and radiological findings*

a. Comparisons among initial imaging modalities

	Imaging modality	Reference modality	OR (95% CI)
Intramural hematoma	HR-3D-T1WI	C-MRI/MRA	4.72 (1.71-13.00)
Double lumen or intimal flap	HR-3D-T1WI	C-MRI/MRA	2.06 (0.60-6.96)
	HR-3D-T1WI	DSA	1.54 (0.49-4.75)
	DSA	C-MRI/MRA	1.34 (0.37-4.79)
Fusiform or irregular aneurysmal dilation	HR-3D-T1WI	C-MRI/MRA	0.80 (0.35-1.84)
	HR-3D-T1WI	DSA	0.86 (0.37-1.97)
	DSA	C-MRI/MRA	0.92 (0.42-2.05)
Pearl-and-string sign	DSA	C-MRI/MRA	2.07 (0.83-5.12)

b. Comparison between initial and follow-up imaging

	Imaging modality	Reference modality	OR (95%CI)
Rapid change in morphology	DSA	C-MRI/MRA	0.67 (0.14-3.10)

Abbreviations: CI, confidence interval; C-MRI/MRA, conventional magnetic resonance imaging and magnetic resonance angiography; DSA, digital subtraction angiography; HR-3D-T1WI, high-resolution 3-dimensional T1-weighted imaging; OR, odds ratio.

Adjusted for multiple evaluations in different modalities and days from symptoms onset to performance of each imaging modality or interval days between initial and follow-up imaging.

We omitted the data of string sign.

Dummy variable was used for analysis of double lumen or intimal flap, fusiform or irregular aneurysmal dilation.

found that IMH decreased from the earlier period to the chronic period (>60 days).[10] However, the interval for repeated imaging was short compared with previous research[10] and another study showed that IMH had the highest signal intensity 4-37 days from onset.[38] Closer re-evaluation may contribute to detection of IMH. Our results also showed the importance of follow-up imaging in the subacute stage for diagnosing IAD.

Recognition and diagnosis of IAD increasingly depends on improved-neurovascular-imaging tools.[39-41] Both C-MRI/MRA and HR-3D-T1WI were noninvasive and effective techniques for vascular evaluation in this research.

Table 9. *Modified Rankin scale score at 3 months after symptoms onset in IAD patients*

a. Sixty-four IAD patients

mRS at 3 months	Patients (n = 64)
0, n (%)	36 (56)
1, n (%)	18 (28)
2-6, n (%)	10 (16)

b. Stroke patients

mRS at 3 months	Patients (n = 38)
0, n (%)	12 (32)
1, n (%)	16 (42)
2-6, n (%)	10 (26)

Abbreviations: IAD, intracranial artery dissection; mRS, modified Rankin scale score.

We found that the rate of observed IMH was significantly higher on HR-3D-T1WI than on C-MRI/MRA sequences at initial imaging. This is because HR-MRI has been proven to have the ability to look beyond the vessel lumen,[41,42] providing direct visualization of the arterial wall in dissection,[12,19] which also enabled us to diagnose dissection present as occlusions, stenosis, or hypoplasia on MRA.[21,43] The fat-suppression technique in HR-3D-T1WI was also helpful in distinguishing fat tissue from IMH including methemoglobin.[44] HR-3D-T1WI has been reported as superior to MRA for evaluating IMH. However, that previous study targeted cases already diagnosed as IAD.[45] Our research showed that HR-3D-T1WI was excellent compared with MRA for detecting IMH in a process to diagnose IAD based on new diagnostic criteria advocated by international experts. Conducting evaluations by including HR-3D-T1WI from the early stage is therefore important.

When we compared initial and follow-up imaging, no significant difference in detecting rapid changes in morphology was evident between C-MRI/MRA and DSA, although DSA offers the ability to obtain images invasively in various projections.[46] This might be influenced by the smaller number of patients able to be followed-up by DSA compared to C-MRI/MRA because diagnostic DSA was relatively invasive. However, the results may suggest that rapid changes in morphology in IAD can be sufficiently evaluated by C-MRI/MRA. The role of DSA in the diagnosis of IAD may be limited to simultaneously providing information on diagnosis and treatment strategies by evaluating image patterns for the vessel lumen.

Our study has some limitations requiring consideration. First, although all documented data except radiological findings were checked by a team of doctors in charge, and in departmental conferences, inclusions were dependent on the registered diagnosis, and our results thus may have included some selection bias. Second, our registry did not contain patients with IAD admitted to the Department of Neurosurgery mainly due to dissection-related subarachnoid hemorrhage. Patients with IAD admitted for the purpose of surgery or endovascular therapy were also seen in the Department of Neurosurgery. Stroke severity in our study was very mild, less likely to be associated with aneurysmal dilation, and thus showing lower rates of headache or neck pain and compressive symptoms. This study was therefore unable to show the relationship between HR-3D-T1WI and pathological findings. Third, we did not compare HR-3D-T1WI with 2-dimensional T1WI, because T1WI was not included in the MRI protocol at the time of emergency admission to the National Cerebral and Cardiovascular Center. However, one of the reports on diagnosing vertebral artery dissection has already noted 3-dimensional black blood T1WI as an excellent tool for detecting intramural hematoma compared with axial T1WI.[45] Fourth, we were not completely able to distinguish intramural hematoma from intraplaque hemorrhage of atheromatous plaque, because intraplaque hemorrhage appeared hyperintense on fat-suppressed T1WI. Finally, T2*-weighted imaging findings of intramural hematoma were not discussed in this study. This was because susceptibility-weighted imaging, which is more sensitive to changes in magnetic susceptibility, has already been discussed in a past study,[47] and intramural hematoma was defined by MRA (axial source images) or HR-3D-T1WI.

Conclusions

In conclusion, we have described the clinical and radiological characteristics of IAD using diagnostic criteria recently proposed by the International expert group on IAD. The predominance of male and middle-aged patients in our study was similar to previous studies, and more than half had hypertension and smoking history. HR-3D-T1WI was suggested to be more useful than C-MRI/MRA in detecting IMH at initial imaging. Additional follow-up imaging enabled about 1 in 5 of our patients to be diagnosed with IAD.

Author Contributions

Yuki Nakamura, study concept and design, acquisition, analysis and interpretation of data, drafting of manuscript

Yoshitaka Yamaguchi, acquisition, analysis and interpretation of data, revision of manuscript for intellectual content

Naoki Makita, acquisition, analysis and interpretation of data

Yoshiaki Morita, study concept

Toshihiro Ide, analysis and interpretation of data

Shinichi Wada, analysis and interpretation of data

Tadataka Mizoguchi, analysis and interpretation of data

Hajime Ikenouchi, analysis and interpretation of data

Kaori Miwa, analysis and interpretation of data

Kenichiro Yi, analysis and interpretation of data

Kenichi Irie, analysis and interpretation of data

Shun Shimohama, revision of manuscript for intellectual content

Masafumi Ihara, study concept and design

Kazunori Toyoda, study concept and design, revision of manuscript for intellectual content

Masatoshi Koga, study concept and design, revision of manuscript for intellectual content, study supervision, financial support

Acknowledgment

We wish to thank Koko Asakura, PhD and Toshimitsu Hamasaki, PhD (statistical assistance).

Conflicts of Interest

We have no disclosures relevant to the manuscript to report.

References

1. De Giuli V, Grassi M, Lodigiani C, et al. Association between migraine and cervical artery dissection: the Italian project on stroke in young adults. JAMA Neurol 2017;74:512-518.
2. Putaala J, Metso AJ, Metso TM, et al. Analysis of 1008 consecutive patients aged 15 to 49 with first-ever ischemic stroke: the Helsinki young stroke registry. Stroke 2009;40:1195-1203.
3. Leys D, Bandu L, Hénon H, et al. Clinical outcome in 287 consecutive young adults (15 to 45 years) with ischemic stroke. Neurology 2002;59:26-33.
4. Sikkema T, Uyttenboogaart M, Eshghi O, et al. Intracranial artery dissection. Eur J Neurol 2014;21:820-826.
5. Ahn SS, Kim BM, Suh SH, et al. Spontaneous symptomatic intracranial vertebrobasilar dissection: initial and follow-up imaging findings. Radiology 2012;264:196-202.
6. Matsukawa H, Shinoda M, Fujii M, et al. Differences in vertebrobasilar artery morphology between spontaneous intradural vertebral artery dissections with and without subarachnoid hemorrhage. Cerebrovasc Dis 2012;34:393-399.
7. Metso TM, Metso AJ, Helenius J, et al. Prognosis and safety of anticoagulation in intracranial artery dissections in adults. Stroke 2007;38:1837-1842.
8. Sato S, Toyoda K, Matsuoka H, et al. Isolated anterior cerebral artery territory infarction: dissection as an etiological mechanism. Cerebrovasc Dis 2010;29:170-177.
9. Hwang J, Chung JW, Cha J, et al. Selective application of high-resolution 3 T MRI in the evaluation of intracranial vertebral artery dissection. J Neuroimaging 2017;27:71-77.

10. Park KJ, Jung SC, Kim HS, et al. Multi-contrast high-resolution magnetic resonance findings of spontaneous and unruptured intracranial vertebral artery dissection: qualitative and quantitative analysis according to stages. Cerebrovasc Dis 2016;42:23-31.
11. Swartz RH, Bhuta SS, Farb RI, et al. Intracranial arterial wall imaging using high-resolution 3-tesla contrast-enhanced MRI. Neurology 2009;72:627-634.
12. Edjlali M, Roca P, Rabrait C, et al. 3D fast spin-echo T1 black-blood imaging for the diagnosis of cervical artery dissection. AJNR Am J Neuroradiol doi: 10.3174/ajnr.A3261.
13. Debette S, Compter A, Labeyrie MA, et al. Epidemiology, pathophysiology, diagnosis, and management of intracranial artery dissection. Lancet Neurol 2015;14:640-654.
14. Park J, Mugler 3rd JP, Horger W, et al. Optimized T1-weighted contrast for single-slab 3D turbo spin-echo imaging with long echo trains: application to whole-brain imaging. Magn Reson Med 2007;58:982-992.
15. Mihai G, Chung YC, Merchant A, et al. T1-weighted-SPACE dark blood whole body magnetic resonance angiography (DB-WBMRA): initial experience. J Magn Reson Imaging 2010;31:502-509.
16. Zhang L, Zhang N, Wu J, et al. High resolution three dimensional intracranial arterial wall imaging at 3 T using T1 weighted SPACE. Magn Reson Imaging 2015;33:1026-1034.
17. Mihai G, Chung YC, Kariisa M, et al. Initial feasibility of a multi-station high resolution three-dimensional dark blood angiography protocol for the assessment of peripheral arterial disease. J Magn Reson Imaging 2009;30:785-793.
18. Li Q, Wang J, Chen H, et al. Characterization of craniocervical artery dissection by simultaneous mr noncontrast angiography and intraplaque hemorrhage imaging at 3T. AJNR Am J Neuroradiol 2015;36:1769-1775.
19. Naggara O, Louillet F, Touzé E, et al. Added value of high-resolution MR imaging in the diagnosis of vertebral artery dissection. AJNR Am J Neuroradiol 2010;31:1707-1712.
20. Kirsch E, Kaim A, Engelter S, et al. MR angiography in internal carotid artery dissection: improvement of diagnosis by selective demonstration of the intramural haematoma. Neuroradiology 1998;40:704-709.
21. Yang WJ, Chen XY, Zhao HL, et al. Postmortem study of validation of low signal on fat-suppressed T1-weighted magnetic resonance imaging as marker of lipid core in middle cerebral artery atherosclerosis. Stroke 2016;47:2299-2304.
22. Han M, Rim NJ, Lee JS, et al. Feasibility of high-resolution MR imaging for the diagnosis of intracranial vertebrobasilar artery dissection. Eur Radiol 2014;24:3017-3024.
23. Drapkin AJ. The double lumen: a pathognomonic angiographic sign of arterial dissection? Neuroradiology 2000;42:203-205.
24. Wang Y, Lou X, Li Y, et al. Imaging investigation of intracranial arterial dissecting aneurysms by using 3 T high-resolution MRI and DSA: from the interventional neuroradiologists' view. Acta Neurochir (Wien) 2014;156:515-525.
25. Matsumoto J, Ogata T, Abe H, et al. Do characteristics of dissection differ between the posterior inferior cerebellar artery and the vertebral artery? J Stroke Cerebrovasc Dis 2014;23:2857-2861.
26. Kawaguchi S, Sakaki T, Tsunoda S, et al. Management of dissecting aneurysms of the posterior circulation. Acta Neurochir (Wien) 1994;131:26-31.
27. Kanda Y. Investigation of the freely available easy-to-use software 'EZR' for medical statistics. Bone Marrow Transplant 2013;48:452-458.
28. Hassan AE, Rostambeigi N, Chaudhry SA, et al. Combination of noninvasive neurovascular imaging modalities in stroke patients: patterns of use and impact on need for digital subtraction angiography. J Stroke Cerebrovasc Dis doi: 10.1016/j.jstrokecerebrovasdis.2012.03.020.
29. Yamaura A, Ono J, Hirai S. Clinical picture of intracranial non-traumatic dissecting aneurysm. Neuropathology 2000;1:85-90.
30. Kang SY, Kim JS. Anterior cerebral artery infarction: stroke mechanism and clinical-imaging study in 100 patients. Neurology 2008;70:2386-2393.
31. Kumral E, Bayulkem G, Evyapan D, et al. Spectrum of anterior cerebral artery territory infarction: clinical and MRI findings. Eur J Neurol 2002;9:615-624.
32. Shin DH, Hong JM, Lee JS, et al. Comparison of potential risks between intracranial and extracranial vertebral artery dissections. Eur Neurol 2014;71:305-312.
33. Hensler J, Jensen-Kondering U, Ulmer S, et al. Spontaneous dissections of the anterior cerebral artery: a meta-analysis of the literature and three recent cases. Neuroradiology 2016;58:997-1004.
34. Virdis A, Taddei S. Endothelial dysfunction in resistance arteries of hypertensive humans: old and new conspirators. J Cardiovasc Pharmacol 2016;67:451-457.
35. Leone A, Landini L. Vascular pathology from smoking: look at the microcirculation! Curr Vasc Pharmacol 2013;11:524-530.
36. Debette S, Metso T, Pezzini A, et al. Association of vascular risk factors with cervical artery dissection and ischemic stroke in young adults. Circulation 2011;123:1537-1544.
37. Zang Y, Wang C, Zhang Y, et al. Long-term follow-up study of 35 cases after endovascular treatment for vertebrobasilar dissecting aneurysms. Clin Neurol Neurosurg 2015;137:121-131.
38. Habs M, Pfefferkorn T, Cyran CC, et al. Age determination of vessel wall hematoma in spontaneous cervical artery dissection: a multi-sequence 3T cardiovascular magnetic resonance study. J Cardiovasc Magn Reson doi: 10.1186/1532-429X-13-76.
39. Provenzale JM, Sarikaya B Comparison of test performance characteristics of MRI, MR angiography, and CT angiography in the diagnosis of carotid and vertebral artery dissection: a review of the medical literature AJR Am J Roentgenol 2009;193:1167-1174.
40. Kobayashi N, Murayama Y, Yuki I, et al. Natural course of dissecting vertebrobasilar artery aneurysms without stroke. AJNR Am J Neuroradiol 2014;35:1371-1375.
41. Swartz RH, Bhuta SS, Farb RI, et al. Intracranial arterial wall imaging using high-resolution 3-tesla contrast-enhanced MRI. Neurology 2009;72:627-634.
42. Jung SC, Kang DW, Turan TN. Vessel and vessel wall imaging. Front Neurol Neurosc 2016;40:109-123.
43. Hwang J, Chung JW, Cha J, et al. Selective Application of High-Resolution 3 T MRI in the Evaluation of Intracranial Vertebral Artery Dissection. J Neuroimaging 2017;27:71-77.

44. Cuvinciuc V, Viallon M, Momjian-Mayor I, et al. 3D fat-saturated T1 SPACE sequence for the diagnosis of cervical artery dissection. Neuroradiology 2013;55: 595-602.
45. Takano K, Yamashita S, Takemoto K, et al. MRI of intracranial vertebral artery dissection: evaluation of intramural haematoma using a black blood, variable-flip-angle 3D turbo spin-echo sequence. Neuroradiology 2013;55:845-851.
46. Hassan AE, Rostambeigi N, Chaudhry SA, et al. Combination of noninvasive neurovascular imaging modalities in stroke patients: patterns of use and impact on need for digital subtraction angiography. J Stroke Cerebrovasc Dis doi: 10.1016/j.jstrokecerebrovasdis.2012.03.020.
47. Kim TW, Choi HS, Koo J, et al. Intramural hematoma detection by susceptibility-weighted imaging in intracranial vertebral artery dissection. Cerebrovasc Dis 2013;36: 292-298.